Antenna Characterization in the Time Domain

Amir Shlivinski, *Member, IEEE*, Ehud Heyman, *Senior Member, IEEE*, and Raphael Kastner, *Senior Member, IEEE*

***Abstract*— A theory for a complete far-field transmit-receive system characterization of short-pulse antennas is derived in the time domain. The transmit-receive antenna system is characterized by a set of cascaded operators, which traPnsform the source waveform and power into similar quantities at the receiving antenna terminals. Two such sets are defined. The first one is phrased in terms of the wave-type "time-dependent effective-height" operator, while the second one is defined in terms of the energy-type "gain operator." Both definitions fit within a complete transmit-receive system description, the latter being equivalent to the frequency-domain Friis equation. However, these operators are derived entirely in the context of the time-domain field equation. The starting point in the time-domain analysis of the effective height is the slant stack transform (SST) of the time-dependent current distribution in a manner equivalent to the spatial Fourier transform used in the frequency domain. The vector autocorrelation of the transmitting effective height is then used to define the time-dependent gain operator under impulsive source excitation. Time-domain reciprocity leads to the definitions of antenna parameters under receiving conditions and the corresponding equivalent circuit. The parameters defined in this way fit within a consistent transmit-receive convolution operator, operating on the autocorrelation of the input signal. This independent time-domain representation is thus similar to the frequency-domain representation. However, unlike the conventional frequency-domain circuit parameters, which relate voltage and current amplitudes, the time-domain circuit representation is based on incident and reflected wave-type constituents. In addition, the use of appropriate norms facilitates the transformation of our operators to stand-alone figures of merits. The general concepts developed herein are demonstrated for the example of the short dipole antenna.**

***Index Terms*—Antennas, transient analysis.**

I. Introduction

THE ever-increasing interest in the radiation and detection of shorter pulses with ultrawideband (UWB) bandwidths has made an impact on time-domain (TD) analysis and design of UWB antennas. In principle, UWB pulses offer possibilities for local high-resolution interrogation of targets or environments and for efficient transfer of localized electromagnetic energy. For a recent review of applications see [1].

One way of analyzing the radiation and detection of these pulses would involve the traditional frequency-domain (FD) antenna parameters on a frequency-by-frequency basis. FD parametrization of the antennas lends itself conveniently to producing a comprehensive transmit-receive system description. However, because of the broad frequency band of the short-pulsed fields, direct treatment of the antennas in the TD may lead to more efficient and physically transparent representations. The dividends of a self-sustained TD description call for a development of a complete characterization of a transmit-receive antenna system. This system characterization should be equivalent to the FD parameters and possess their important features, in particular, the ability to link all parts of the transmit-receive system together, in a manner equivalent to the FD Friis equation. As shown below, contrary to FD antenna parametrization, the TD characterization is based on integral operators, which can be cast both in terms of wave-like, as well as power quantities. In both cases, these operators fit within the desired description of the system. For the case of power-related operators, we arrive at a formulation analog to the FD Friis equation.

Analysis [2], [3] and optimization [4]–[8] of the radiated pulsed energy in a given direction have been performed in the TD, however, without resorting to TD characterization. A class of TD definitions of the antenna gain as a numerical parameter has been introduced in [9]–[12]. These definitions closely follow the philosophy of the FD definitions, and are based on a norm of the radiation at a certain direction normalized to the spatial average of the radiated power. Other definitions, which can be found in [13]–[16], also follow the spirit of the FD concepts. The norm-based definitions serve to characterize an antenna in the TD as stand-alone concepts rather than being incorporated into a complete transmit-receive system such as the Friis equation.

In this paper, we address the antenna characterization entirely in the TD starting with the transmitting antenna in Section II. It is first shown that the far field is derived from the current distribution directly in the TD using the slant stacked transform (SST) [17]–[21]. The SST proves to be a fundamental tool in TD analysis, and is equivalent to the spatial Fourier transform of the current distribution used to evaluate the far field in the FD. The far field is expressed systematically in terms of the effective height operator, which is a characteristic of the antenna, used with the source waveform to produce the far field via a convolution integral. This operator is found by performing the SST of the time-dependent current distribution. As an example (Section V and Appendix B), the SST is used to calculate the effective height of a short dipole, yielding a temporal differentiation operator, as expected [13].

The TD system operators are defined with reference to the current-wave incident upon the antenna terminals. The link to total amplitudes, which serve as a references in FD definitions, is addressed in Appendix A and involves the FD reflection coefficient. The effective height is thus considered a wave-type quantity, which later (Section IV) fits within the complete transmit-receive wave-type relationship. In addition, an energy-type system representation (such as the FD Friis

Manuscript received March 1, 1996; revised December 2, 1996.

The authors are with Department of Electrical Engineering, Physical Electronics, Tel-Aviv University, Tel-Aviv, 69978 Israel.

Publisher Item Identifier S 0018-926X(97)04895-3.

equation) requires the definition of the TD antenna "gain operator." This energy-type operator is defined via a vector autocorrelation of the far field, normalized to the average available energy. It can, therefore, be evaluated from the autocorrelation of the TD transmitting antenna effective height. A related definition, derived from the gain operator, is a figure of merit called the "gain parameter," that parametrizes the overall energy transmission properties of the system for a given excitation waveform.

In Section III, the receiving antenna is characterized. Using TD reciprocity [21], [22], the effective height of the receiving antenna is shown to be a temporal-integration of the effective height for the antenna in the transmitting mode. This statement is analogous to the identity of the transmitting and receiving patterns in the FD. Taking the receiving antenna circuit into account, we arrive at the TD transmit-receive antenna system description in Section IV. The system is described by a succession of convolution integrals, for both the wave-type and the energy-type equations. The wave-type representation involves the effective height operating on the input signal. The energy-type equation involves the gain operators operating on the autocorrelation of the input signal. Its FD counterpart is a numerical parameter, appearing in the Friis equation as a multiplier of the power spectrum of the source. In this way, the system has been described entirely in the TD in a coherent way, using the slant-stacked transform to produce characteristic operators whose interaction forms the final system equation. These new formulas are demonstrated by an example of the short dipole in Section V and Appendix B. In Appendix A, the full equivalence between the TD and FD parameters and relationships is established, as stated in the conclusion (Section VI).

II. Characterization of Transmitting Antennas

A. Radiation from Impressed Sources

We consider the transmitting antenna configuration in Fig. 1. The input current wave incident at the antenna terminals $I^+(t)$ is assumed to be a short pulse of length T: its relation to the excitation voltage source $V_g(t)$ will be considered in Section II-C. Assuming an impressed current distribution $\mathbf{J}(\mathbf{r},t)$ on the antenna surface, the radiating vector potential $\mathbf{A}(\mathbf{r},t)$ is given by the retarded potential integral

$$\mathbf{A}(\mathbf{r},t) = \mu \int dV' \frac{\mathbf{J}(\mathbf{r}', t - |\mathbf{r}-\mathbf{r}'|/c)}{4\pi|\mathbf{r}-\mathbf{r}'|} \tag{1}$$

where $c = 1/\sqrt{\mu\epsilon}$ is the speed of light in the medium. We are primarily interested in the far zone, hence, we may use in (1)

$$|\mathbf{r}-\mathbf{r}'| \simeq r - \hat{\mathbf{r}}\cdot\mathbf{r}' + \frac{1}{2}\frac{r'^2}{r}[1-(\hat{\mathbf{r}}\cdot\hat{\mathbf{r}}')^2] + \cdots \tag{2}$$

where $r = |\mathbf{r}|$ and $\hat{\mathbf{r}} = \mathbf{r}/r$, with similar definitions for the source coordinate $\mathbf{r}'$. To define the far-zone characteristic operators, we would like to approximate the delay term in (1) by neglecting the last term in (2), which depends on both the observation direction $\hat{\mathbf{r}}$ and on the distance r. This approximation can be effected only if the maximum delay introduced by this term is much smaller than the pulselength T, i.e., if

$$L^2/r \ll cT \tag{3}$$

where L is the source dimension. Note that this "time-domain Fraunhofer condition" (3) becomes identical to the conventional FD condition upon the substitution $\omega = 1/T$, which is the typical upper frequency associated with the excitation pulse. Keeping only the first two terms of (2) in the numerator of (1), and only the first term in the denominator, we obtain the following expression for the pulsed radiation field

$$\mathbf{A}(\mathbf{r},t) \simeq \frac{\mu}{4\pi r}\tilde{\mathbf{J}}(\hat{\mathbf{r}},\tau), \quad \tau = t - r/c \tag{4}$$

where

$$\tilde{\mathbf{J}}(\hat{\mathbf{r}},\tau) = \int dV' \mathbf{J}(\mathbf{r}', \tau + \hat{\mathbf{r}}\cdot\mathbf{r}'/c). \tag{5}$$

The operation in (5) is termed the *slant stack transform* (SST). To gain further insight into this operation we note that the volume integration can be expressed as a cascaded two-step process

$$\mathcal{P}_{\hat{\mathbf{r}}}[\mathbf{J}](\sigma,\tau) = \int d^2r' \mathbf{J}(\mathbf{r}',\tau)|_{\mathbf{r}'\cdot\hat{\mathbf{r}}=\sigma} \tag{6}$$

$$\tilde{\mathbf{J}}(\hat{\mathbf{r}},\tau) = \int d\sigma \mathcal{P}_{\hat{\mathbf{r}}}[\mathbf{J}](\sigma, \tau+\sigma/c). \tag{7}$$

From (6), $\mathcal{P}_{\hat{\mathbf{r}}}[\mathbf{J}](\sigma,\tau)$ is a projection of the time-dependent distribution $\mathbf{J}(\mathbf{r},t)$ onto the direction $\hat{\mathbf{r}}$, obtained by integrating $\mathbf{J}$ along the planes $\mathbf{r}'\cdot\hat{\mathbf{r}} = \sigma$ normal to $\hat{\mathbf{r}}$, where σ is the distance from the origin along the $\hat{\mathbf{r}}$ direction. These projections are subsequently stacked in (7) by integrating along the propagation direction $\hat{\mathbf{r}}$ with a progressive delay σ/c corresponding to the wave speed c (see Fig. 2). This operation, therefore, extracts from the source distribution $\mathbf{J}(\mathbf{r},t)$ the transient plane-wave information that propagates in the $\hat{\mathbf{r}}$ direction. It should be noted that the operation in (5) does not constitute the full transform as it projects the four-dimensional (4-D) $(\mathbf{r},t)$ domain onto a three-dimensional (3-D) subdomain $(\hat{\mathbf{r}},\tau)$. In the full transform, the slant-stack speed is another spectral variable [20]: it is given by (5) with c replaced by the spectral speed $v \in [0,\infty)$. In this sense, the slant-stack transform in the TD plays an analogous role to the spatial Fourier representation in the FD, wherein only spectral contributions on the Ewald sphere $\mathbf{K} = \omega/c$ are retained out of the entire 3-D spectral domain (see Appendix A). A discussion of the full space-time transform and its inverse, as well as its relation to a 4-D Radon transform is given in [20]. Equations (4) and (5) are thus the ones to be used for far-field calculations in the TD. In analogy with the Fourier transform in the FD (see Appendix A), they imply the following: 1) the far field consists only of the plane-wave constituents that propagate with the speed of light c and 2) the field in the $\hat{\mathbf{r}}$ direction is described by the transient plane wave that propagates in that direction.

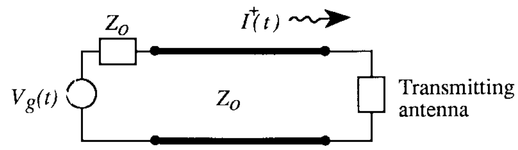

Fig. 1. The radiating antenna circuit.

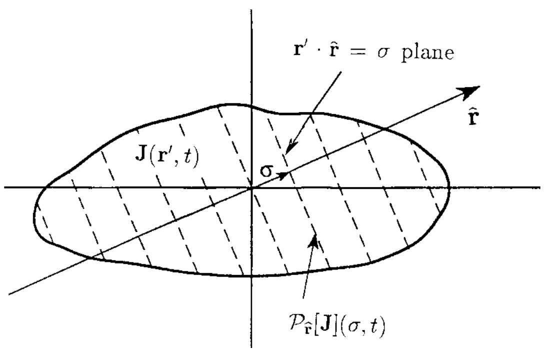

Fig. 2. The slant-stack transform of the current distribution $\mathbf{J}(\mathbf{r}, t)$.

B. Effective Height of a Transmitting Antenna

The effective height of the transmitting antenna $\mathbf{h}^t$ (in units of [m/s^2]) defines the relationship between the forward propagating input current wave at the antenna terminals $I^+(t)$ and the electric field in the far zone via the following convolution integral:

$$\mathbf{E}(\mathbf{r}, t) = -\frac{\mu}{4\pi r}[I^+(\cdot) * \mathbf{h}^t(\hat{\mathbf{r}}, \cdot)](\tau), \qquad \tau = t - r/c \quad (8)$$

where we use the notation $[f(\cdot) * g(\cdot)](t) = \int dt' f(t')g(t-t')$. The effective height is thus the far-field impulse response of the transmitting antenna. Note that in contrast to the FD definition [see (51)], we define the TD effective height with respect to $I^+(t)$ rather than with respect to the total current $I(t)$ since the latter also includes the reflected waveform, including multiple reflections off the antenna structure, etc. In analogy to the far field in the FD, the effective height is independent of the distance and of the actual delay. The free-space spherical wave delay and decay are described by $\tau = t - r/c$ and by the $1/r$ factor in (8).

To calculate the effective height we note that the electric field in the far zone is related to $\mathbf{A}$ via

$$\mathbf{E}(\mathbf{r}, t) = -\partial_t \mathbf{A}_{||}(\mathbf{r}, t) \quad (9)$$

where $\mathbf{A}_{||}(\mathbf{r}, t) = \mathbf{A} - \hat{\mathbf{r}}(\hat{\mathbf{r}} \cdot \mathbf{A})$. Using (4) and (9) we find that the effective height can be cast in the following form:

$$\mathbf{h}^t(\hat{\mathbf{r}}, \tau) = \partial_\tau \int dV' \mathbf{J}^\delta_{||}(\mathbf{r}', \tau + \hat{\mathbf{r}} \cdot \mathbf{r}'/c) \quad (10)$$

where $\mathbf{J}^\delta$ (in units of [1/m^{2}sec]) is the current distribution due to an impulsive input current $I^+(t) = \delta(t)$ and the subscript $||$ denotes the transverse component relative to the observation direction $\hat{\mathbf{r}}$. Evaluation of (10) thus requires an electromagnetic solution of the antenna structure resulting in $\mathbf{J}^\delta(\mathbf{r}, t)$. In the general case, $\mathbf{J}^\delta$ needs to be calculated numerically, e.g., via the finite-difference time-domain (FDTD) technique, however, for electrically small antennas (i.e., ones that are small compared with the pulse length) some simple assumptions may apply, though they may introduce an error within the higher frequency content of the pulse. Note that if the excitation pulses are band-limited within some frequency range, it is sufficient to calculate $\mathbf{J}^\delta$ only for a band-limited impulse whose spectrum is a unity within the relevant frequency range and zero elsewhere. Note also that if $\mathbf{J}^\delta$ has a compact support in space–time, so has $\mathbf{h}^t(\hat{\mathbf{r}}, \tau)$.

C. The Transmitting Antenna Circuit

Referring to the antenna system in Fig. 1, we shall assume that the antenna is connected to a uniform line with frequency independent characteristic impedance Z_0. Although not shown explicitly, the circuit model in Fig. 1 may include matching elements between the transmission line and the antenna terminals or at the source. Typically, these elements create multiple reflections between themselves and the antenna terminals or the source. In a single-frequency scenario, the matching elements can be tuned up in order to adjust the phase produced by the summation of the infinite series of multiple reflections so as to offset the reflected wave along the main transmission line. Such impedance matching is thus essentially band limited. Under ultrawideband/short-pulse conditions, on the other hand, the series consists also of successive pulse delays (as well as possible pulse distortions due to reactive elements) and, in general, cannot be lumped into a single parameter such as a reflection coefficient in the TD. We may, therefore, assume that the antenna is *not matched* and its terminals are connected directly to the line as depicted in Fig. 1. We shall also assume that the source impedance R_g is purely resistive. To eliminate multiple reflections along the main transmission line, R_g should be set equal to Z_0, however, this restriction may easily be removed by standard techniques. Referring to the antenna system in Fig. 1, $I^+(t)$ in (8) is, therefore, related to the source voltage $V_g(t)$ via

$$I^+(t) = V_g(t - t_g)/2Z_0 \quad (11)$$

where t_g is the time delay along the input line. From (8), the radiated field at the far-field zone is thus given by

$$\mathbf{E}(\mathbf{r}, t) = -\frac{c^{-1}}{8\pi r}\frac{\eta}{Z_0}[V_g(\cdot) * \mathbf{h}^t(\hat{\mathbf{r}}, \cdot)](\tau - t_g) \quad (12)$$

where $\eta = \sqrt{\mu/\epsilon}$ is the wave impedance.

D. Time-Dependent Gain Operator of a Transmitting Antenna

The TD gain may be considered from two different viewpoints—in the first way, one is interested in a *time-independent* parameter that describes the radiation characteristics in a given direction. This "gain parameter" is defined by taking an appropriate norm of (12). Here, we shall consider only the energy (or $\mathcal{L}_2$) norm, however, the definitions and operations used can be extended to other norms [9]–[12] (e.g., the ∞ norm that extracts the peak value of the signals). The second definition is designed to fit within a complete description of a transmit-receive system, discussed below, wherein the specific antenna is only a subsystem. The antenna gain concept in this case is a time-dependent function which we may term the "gain operator." Within the framework of energy $(\mathcal{L}_2)$ norms, the gain operator is an autocorrelation function out of which the energy-gain parameter can be extracted by taking the value of the gain operator for a given pulse at $t = 0$. When the antenna is incorporated as a subsystem in a complete system that may involve additional time-dependent operations, the *global* gain operator, and thereby the *global* energy-gain parameter will be found by convolving the gain operators of the various subsystems. For later use, we specify below definitions of the autocorrelation and the energy norm of a time-dependent (deterministic) signal $X(t)$ as

$$\mathcal{R}_X(\xi) = \int dt X(t)X(t-\xi), \qquad \|X(\xi)\|^2 = \mathcal{R}_X(0) \quad (13)$$

respectively.

The general considerations mentioned above are applied next to the transmitting antenna subsystem. We shall normalize the gain with respect to the maximum available energy from the source

$$\mathcal{E}_g = \frac{1}{4}\frac{\|V_g\|^2}{Z_0}, \qquad Z_0 = R_g. \quad (14)$$

The transmitting antenna gain operator $\mathbf{g^t}(\hat{\mathbf{r}}, \xi)$ is defined now via

$$\frac{1}{\eta}\mathcal{R}_{\mathbf{E}}(\mathbf{r}, \xi) = \frac{\mathcal{E}_g}{4\pi r^2}[\mathbf{g}^t(\hat{\mathbf{r}}, \cdot) * \bar{\mathcal{R}}_{V_g}(\cdot)](\xi) \quad (15)$$

where $\mathcal{R}_{\mathbf{E}}(\mathbf{r}, \xi)$ is the vector autocorrelation of $\mathbf{E}(\mathbf{r}, t)$, whose components are the autocorrelation of corresponding components of $\mathbf{E}(\mathbf{r}, t)$ i.e., $\mathcal{R}_{\mathbf{E}}(\mathbf{r}, \xi) = \hat{\mathbf{x}}\mathcal{R}_{E_x}(\mathbf{r}, \xi) + \hat{\mathbf{y}}\mathcal{R}_{E_y}(\mathbf{r}, \xi) + \hat{\mathbf{z}}\mathcal{R}_{E_z}(\mathbf{r}, \xi)$. In (15), $\mathbf{g^t}$ operates on

$$\bar{\mathcal{R}}_{V_g}(\xi) \equiv \mathcal{R}_{V_g}(\xi)/\mathcal{R}_{V_g}(0) \quad (16)$$

which is the normalized autocorrelation of $V_g(t)$ (note that $\mathcal{R}_{V_g}(0) = \|V_g\|^2$). Upon combining (8), (12), and (14), one obtains

$$\mathbf{g}^t(\hat{\mathbf{r}}, \xi) = \frac{1}{4\pi c^2}\frac{\eta}{Z_0}\mathcal{R}_{\mathbf{h}^t}(\hat{\mathbf{r}}, \xi), \qquad [\mathrm{s}^{-1}] \quad (17)$$

where $\mathcal{R}_{\mathbf{h}^t}(\hat{\mathbf{r}}, \xi)$ is the vector autocorrelation of $\mathbf{h}^t(\hat{\mathbf{r}}, \tau)$ of (10). As mentioned above, the antenna may now be parametrized conveniently in terms of the energy-gain parameter defined by

$$G^t(\hat{\mathbf{r}}) = |\bar{\mathcal{R}}_{V_g}(\xi) * \mathbf{g}^t(\hat{\mathbf{r}}, \xi)|_{\xi=0}. \quad (18)$$

This parameter provides a *time-independent* radiation pattern. However, it cannot be incorporated into a complete transmit-receive system representation that involves additional TD operations.

III. System Characterization of a Receiving Antenna

A. Effective Height of a Receiving Antenna

Referring to Fig. 3, and following the general TD strategy outlined in the Introduction, we shall be interested in the traveling wave $V^{-}(t)$ obtained when the antenna terminals are connected to a line with a frequency-independent characteristic impedance Z_0 terminated by a matched load $R_L = Z_0$. It is assumed that the incident field is a pulsed plane wave

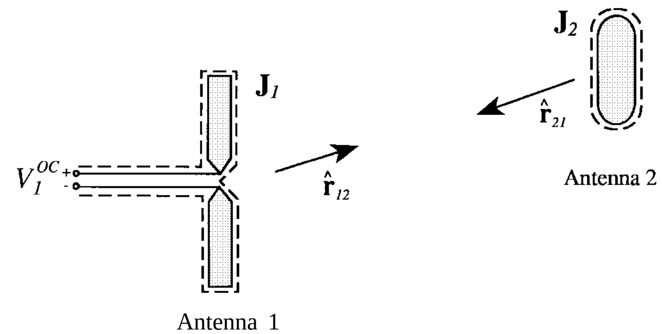

Fig. 3. Time-domain reciprocity applied to a transmit-receive configuration.

$$\mathbf{E}^i(\mathbf{r}, t) = \mathbf{E}_0(t - \hat{\mathbf{r}}^i \cdot \mathbf{r}/c) \quad (19)$$

where $\mathbf{E}_0(t)$ has an arbitrary waveform and is polarized perpendicular to the propagation direction $\hat{\mathbf{r}}^i$. The TD effective height of the receiving antenna is thus defined via

$$V^{-}(t) = -[\mathbf{E}_0(\cdot) \star \mathbf{h}^r(\hat{\mathbf{r}}, \cdot)](t) \quad (20)$$

where $\star$ denotes a temporal convolution concurrent with spatial scalar product.

Using TD reciprocity theorem, it is now feasible and convenient to characterize the receiving antenna using its description in the transmission mode. We consider the transmit-receive antenna configuration in Fig. 3 with current distributions $\mathbf{J}_1$ and $\mathbf{J}_2$ for the receiving antenna 1 and the auxiliary transmitting antenna 2, respectively. The TD reciprocity theorem applies to independent sources and their fields in the presence of an arbitrary reciprocal medium (not necessarily free space, e.g., it may consist of impedance boundaries and lossy media) and can be phrased, for an infinite volume as follows [22]:

$$\int_{V_1} dV \int dt \mathbf{J}_1 \cdot \mathbf{E}_2^\dagger = \int_{V_2} dV \int dt \mathbf{J}_2^\dagger \cdot \mathbf{E}_1 \quad (21)$$

where $\mathbf{E}_1$ is the field due to $\mathbf{J}_1$ while $\mathbf{E}_2^\dagger$ is the adjoint field due to $\mathbf{J}_2^\dagger$. V_1 and V_2 are the supporting volumes of $\mathbf{J}_1$ and $\mathbf{J}_2$, respectively. The adjoint field is defined as obeying a set of equations similar to Maxwell's, except for a sign reversal for both $\partial/\partial t$ and ∇. The adjoint current $\mathbf{J}_2^\dagger$ is considered zero from a certain time on (as opposed to $\mathbf{J}_1$ which is zero up to a certain time). These adjoint sources and fields are related by noncausal Green's functions, e.g., the adjoint potential $\mathbf{A}_2^\dagger$ in free space is given by [compare (1)]

$$\mathbf{A}_2^\dagger(\mathbf{r}, t) = \mu \int_{V_2} dV' \frac{\mathbf{J}_2^\dagger(\mathbf{r}, t + |\mathbf{r} - \mathbf{r}'|/c)}{4\pi|\mathbf{r} - \mathbf{r}'|}. \quad (22)$$

The adjoint field are then calculated from $\mathbf{A}_2^\dagger$ via $\mu\mathbf{H}_2^\dagger = -\nabla \times \mathbf{A}_2^\dagger$ (note the $-$ sign which does not appear in the causal system).

As depicted in Fig. 3, the left-hand side integration in (21) will be performed over the independent sources $\mathbf{J}_1$ within a volume V_1. These sources can be defined in two ways, according to the definition of the medium that surrounds them. In the first definition, $\mathbf{J}_1$ is the source at the antenna terminal

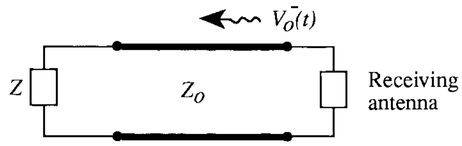

Fig. 4. The receiving antenna circuit.

hence the antenna structure is considered to be a part of the medium and $\mathbf{E}_2$ is computed in the presence of the antenna structure. Thus, the left-hand side in (21) yields

$$\int dtI_1(t)\int_{(1)^-}^{(1)^+} d\mathbf{s}\cdot\mathbf{E}_2^{\dagger}(\mathbf{r},t) = -\int dtI_1(t)V_1^{\mathrm{oc}^\dagger}(t) \tag{23}$$

where the $d\mathbf{s}$ line integration on the left-hand side is performed between the terminals $(1)^-$ and $(1)^+$, and $I_1(t)$ is the input current. The open circuit voltage $V_1^{\mathrm{oc}^\dagger}$ is obtained from the left-hand side via $V_1^\dagger(t) = -\int_{(1)^-}^{(1)^+}\mathbf{E}_2^\dagger(\mathbf{r},t)\cdot d\mathbf{s}$ by noting that $\mathbf{E}_2$ is the open-circuit field ($\mathbf{E}_2$ is the field due to I_2 with $I_1 = 0$).

We now use the fact that the input current when antenna 1 is transmitting is given by

$$I_1(t) = \left[\delta(t) - \Gamma_1^t(t)\right] * I_1^+(t) \tag{24}$$

where $\Gamma_1^t(t)$ is the time-dependent reflected waveform due to an impulsive input voltage at the antenna terminals ($\Gamma_1^t(t)$ is the inverse Fourier transform of the FD reflection coefficient $\hat{\Gamma}^t(\omega)$ used in Appendix A). Referring to the receiving antenna equivalent circuit in Fig. 4 we also note that

$$[\delta(t) - \Gamma_1^t(t)] * V_1^{\mathrm{oc}}(t) = 2V_1^-(t). \tag{25}$$

Thus, substituting (24) and (25) into (23), and noting that $V_1^{\mathrm{oc}^\dagger}(t) = V_1^{\mathrm{oc}}(-t)$, the right-hand side of (23) can be written as $-2\int dt\ I_1^+(t)V_1^-(-t)$. Further, using (20), we obtain $2\int dt\ I_1^+(t)\int dt'\ \mathbf{E}_0(t')\cdot\mathbf{h}_1^r(\hat{\mathbf{r}}_{12}, -t-t')$ and, finally, (23) becomes

$$2\int dt\mathbf{E}_0(t)\cdot\left[\mathbf{h}_1^r(\hat{\mathbf{r}}_{12},\cdot) * I_1^+(\cdot)\right](-t). \tag{26}$$

The second definition of $\mathbf{J}_1$ includes the induced current over the antenna structure as an independent source, which implies that $\mathbf{J}_1$ is assumed to be radiating in free space. In this case, $\mathbf{E}_2$ is simply the incident field $\mathbf{E}_2^i$ which is assumed to be the pulsed plane wave in (19) (with $\hat{\mathbf{r}}^i = \hat{\mathbf{r}}_{21}$, the unit vector direction from antenna 2 to 1). Thus, using $\mathbf{E}_2^{i^\dagger} = \mathbf{E}_0(-t - \hat{\mathbf{r}}_{21}\cdot\mathbf{r}/c)$ and also $\hat{\mathbf{r}}_{21} = -\hat{\mathbf{r}}_{12}$, the left-hand side in (21) now yields

$$\begin{aligned}\int dt\int_{V_1} dV\mathbf{J}_1(\mathbf{r},t)\cdot\mathbf{E}_2^{i^\dagger}(\mathbf{r},t)&\\ = \int dt\mathbf{E}_0(t)\cdot\int_{V_1} dV\ \mathbf{J}_{||_1}(\mathbf{r}, -t+\hat{\mathbf{r}}_{12}\cdot\mathbf{r}/c).&\end{aligned} \tag{27}$$

where $\mathbf{J}_{||_1}$ is the component of $\mathbf{J}_1$ transverse to $\hat{\mathbf{r}}_{12}$. Using (10), the right-hand side of (27) becomes

$$\int dt\mathbf{E}_0(t)\cdot\left[\partial_t^{-1}\mathbf{h}_1^t(\hat{\mathbf{r}}_{12},\cdot) * I_1^+(\cdot)\right](-t) \tag{28}$$

where ∂_t^{-1} denotes an integration. Noting that (26) and (28) are two alternative forms derived from the left-hand side in (21) and equating these expressions, taking into account the fact $\mathbf{E}_0(t)$ and $I_1^+(t)$ are arbitrary pulses, we obtain the final result

$$\frac{1}{2}\mathbf{h}^t(\hat{\mathbf{r}},t) = \partial_t\mathbf{h}^r(\hat{\mathbf{r}},t). \tag{29}$$

B. The Receiving Antenna Circuit

Referring to Fig. 4, the load current is given by

$$I_L(t) = V^-(t-t_L)/Z_0 \tag{30}$$

where t_L is the propagation delay along the line and it is also assumed, for the sake of simplicity, that $Z = Z_0$. For a given incident pulse $\mathbf{E}_0(t)$, the voltage V^- is given by combining (20) and (29), hence

$$I_L(t) = -\frac{1}{2Z_0}\left[\mathbf{h}^t(\hat{\mathbf{r}},\cdot)\star\partial_t^{-1}\mathbf{E}_0(\cdot)\right](t-t_L) \tag{31}$$

where $\star$ has been defined after (20). Note that the integration and the convolution operators in (31) can commute, e.g., they may be expressed as $[(\partial_t^{-1}\mathbf{h}^t)\star\mathbf{E}_0](t-t_L)$.

IV. A Transmit-Receive Antenna System

Next, we consider a system consisting of a transmitting and a receiving antennas denoted, respectively, by subscripts T and R (Fig. 5). It is assumed that the distance between the antennas is large so that the far-zone models apply. The unit vector directions from antenna T to R and from antenna R to T are denoted, respectively, as $\hat{\mathbf{r}}_{TR}$ and $\hat{\mathbf{r}}_{RT}$. Combining (12) and (31) we obtain for the receiver load current

$$\begin{aligned}I_L(t) = \frac{1}{4\pi r}\frac{c^{-1}\eta}{4Z_{0_T}Z_{0_R}}\big[\big(\mathbf{h}_T^t(\hat{\mathbf{r}}_{TR},\cdot)\star\mathbf{h}_R^t(\hat{\mathbf{r}}_{RT},\cdot)\big)&\\ *\,\partial_t^{-1}V_g(\cdot)\big](\tau - t_g - t_L)&\end{aligned} \tag{32}$$

where $\tau = t - r/c$ and, as mentioned earlier, the ∂_t^{-1} and the convolution operations may commute. Note that we used (29) to express the effective reception height of the receiving antenna $\mathbf{h}_R^r$ in terms of its effective transmission height $\mathbf{h}_R^t$. The energy transmitted to the load $\mathcal{E}_L = \|I_L(t)\|^2R_L$, with $R_L = Z_{0_R}$, may readily be calculated from (32). After a few manipulations, we arrive at

$$\mathcal{E}_L = P_L(\xi)|_{\xi=0} \tag{33}$$

where $P_L(\xi)$ is an energy correlator

$$P_L(\xi) = \mathcal{T}(\xi) * (\mathcal{E}_g\bar{\mathcal{R}}_{V_g}(\xi)) \tag{34}$$

with $\mathcal{T}(\xi)$ being a standard (Friis-type) transmission operator

$$\mathcal{T}(\xi) = -\left(\frac{1}{4\pi r}\right)^2(2\pi c)^2\mathbf{g}_T^t(\hat{\mathbf{r}}_{TR},\xi)\star\mathbf{g}_R^t(\hat{\mathbf{r}}_{RT},\xi)\partial_\xi^{-2}. \tag{35}$$

Here, $\mathcal{E}_g$ is the maximum available energy of the source (14), $\bar{\mathcal{R}}_{V_g}(\xi)$ is the normalized autocorrelation of the source pulse (15) (hence, $\mathcal{E}_g\bar{\mathcal{R}}_{V_g}(\xi)$ is the nonnormalized autocorrelation of the source), and $\mathbf{g}^t(\hat{\mathbf{r}},\xi)$ is the transmission-mode normalized gain operator as given in (17). The relation of (35) and

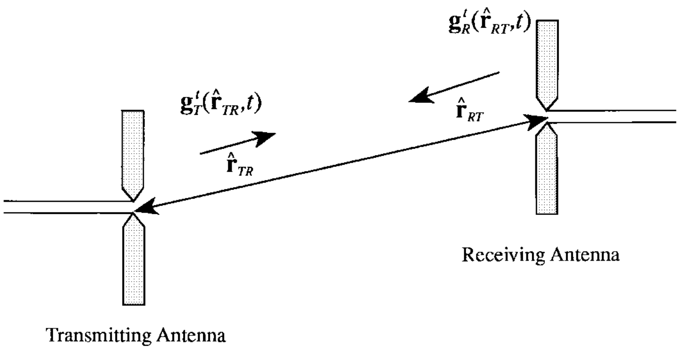

Fig. 5. Time-domain transmit-receive antenna system. The subscripts T and R correspond to the transmitting and receiving antennas, while the superscripts t and r describe the transmission or receive mode of the corresponding antenna. $\hat{\mathbf{r}}_{TR}$ and $\hat{\mathbf{r}}_{RT}$ are unit vector directions from antenna T to R and from antenna R to T, respectively.

(33) to the FD transmit-receive equation (Friis Equation) is discussed in Appendix A. Equation (35) serves to characterize the transmit-receive antenna system fully in terms of energy-related concepts and, as such, it complements the wave related concepts of transmitting and receiving effective height discussed above. It engulfs the analogs of the most popular FD concepts, such as the gains of both transmitting and receiving antennas. The effective aperture concept is also implicit in this formulation; in the frequency domain, it is $\lambda^2/4\pi$ times the gain. In analogy, the two temporal integrations in (35) are equivalent to the λ^2 factor.

Equations (32), (34), and (35) also point the way to measurement of the effective height and the gain operators (it is sufficient to measure only one of them). The received signal (say $I_L(t)$) needs to be measured as a temporal function. Knowing the source term $V_g(t)$, the transmission operator $[\mathbf{h}_T^t(\hat{\mathbf{r}}_{TR},\cdot) \star \mathbf{h}_R^t(\hat{\mathbf{r}}_{RT},\cdot)](t)$ and, subsequently, $\mathbf{h}_T^t(\hat{\mathbf{r}}_{TR},t)$ can be evaluated via a cascaded deconvolution process. The measurement antenna response $\mathbf{h}_R^t(\hat{\mathbf{r}}_{RT},t)$ can be calibrated out using either one of the following techniques: 1) by performing the measurement with a known reference antenna of higher bandwidth relative to the measured antenna or 2) by using two identical antennas for transmit and receive and positioning them such that the pointing angles are the same (relative to their own frames of references) so that (35) becomes an autoconvolution. The gain operator $\mathbf{g}_T^t(\hat{\mathbf{r}}_{TR},\xi)$ can then be recovered from $\mathbf{h}_T^t(\hat{\mathbf{r}}_{RT},t)$ via (17). Alternatively, one may autocorrelate $I_L(t)$ to obtain $P_L(\xi)$ and then extract $\mathbf{g}_T^t(\hat{\mathbf{r}}_{TR},\xi)$ via (34) and (35). In either way, the energy level $\mathcal{E}_g$ and the distance can be calibrated out by using a known reference antenna.

The measurements above can be done directly in the TD, while the data may be processed either in the TD or in the FD. Alternatively, the measurements could be done in a swept-frequency mode but this requires coherent measurement of both amplitude and phase information over the entire frequency range (e.g., using a vector network analyzer).

V. Example: A Short Dipole System

To clarify the physical interpretation of the various quantities introduced, and to demonstrate how they can be calculated and used, we shall consider (below) an antenna system consisting of two dipoles. It will be assumed that the dipole length L is short with respect to the pulse length $L \ll cT$, and also that the dipole diameter $2a$ is much smaller than L. Under these conditions the FD input impedance of the dipole can be approximated by a series combination of the radiation resistance and a capacitance given, respectively, by [22, Section 14.05]

$$R^{\rm rad} = 15(\omega L/c)^2, \qquad C = \frac{\pi}{2\eta c}\frac{L}{\ln(L/2a)}. \tag{36}$$

These expressions have been derived via the induced EMF method. However, to enhance the physical insight into the TD results, it might be helpful to note that the same expression for C may be obtain if one considers the input impedance to an open circuited transmission line with a characteristic impedance $120\ln(L/2a)$ [22, Sections 11.13, 11.14]. It also follows that the short-dipole condition $L \ll cT$ implies $R^{\rm rad} \ll 1/\omega C$ over the entire frequency band $\omega \sim T^{-1}$. In the numerical example below we shall use $L = 1$ m and $a = 1$ cm, so that $R^{\rm rad} = \omega^2 1.66\,10^{-16}$ Ω and $C = 3.55$ pF. We shall consider a Gaussian excitation pulse

$$V_g(t) = (\sqrt{2\pi}T)^{-1/2}e^{-(t/2T)^2} \tag{37}$$

normalized to have a unit energy $||V_g||^2 = 1$ and an rms width T such that $T^2 = (\int_{-\infty}^{\infty} dt\ t^2 V_g^2(t))/||V_g||^2$. We shall use $T = 33$ n sec (i.e., $cT = 10$ m) which complies with the short-dipole approximation.

The TD effective height $\mathbf{h}^t$ is calculated via (10) from the current distribution $\mathbf{J}^\delta$ due to an impulsive input current. Clearly, the high-frequency components in this input pulse are beyond the short-dipole range, but nevertheless we shall evaluate a synthetic "impulse response" by extending the short-dipole approximation to the entire frequency range. When convolved with the physical input pulse, this synthetic "impulse response" provides the correct response provided that the input pulse is within the range of the short-dipole approximation. Under the assumption above, the dipole impulse current $\mathbf{J}^\delta$ takes on the form

$$\mathbf{J}^\delta(z,t) = \begin{cases} \delta(t \mp z/c)\hat{\mathbf{z}}, & \text{for } 0 < t < \frac{1}{2}L/c \\ -\delta(t-(L \mp z)/c)\hat{\mathbf{z}}, & \text{for } \frac{1}{2}L/c < t < L/c \\ 0, & \text{otherwise} \end{cases} \tag{38}$$

where the upper and lower signs apply for the upper and lower arms of the dipole, respectively, $(0 < z < \frac{1}{2}L$ and $-\frac{1}{2}L < z < 0)$. This expression describes a pulse traveling along the dipole arms from the input terminal toward the end points for $0 < t < \frac{1}{2}L/c$ and a reflected pulse for $\frac{1}{2}L/c < t < L/c$, with a -1 reflection coefficient. The analogous distribution in the FD is a triangular one, as shown in Appendix A-F. As mentioned above, we extend the low-frequency approximation to the entire frequency range and neglect the radiation loss along the line. This synthetic model provides a valid result after convolving with the physical signal.

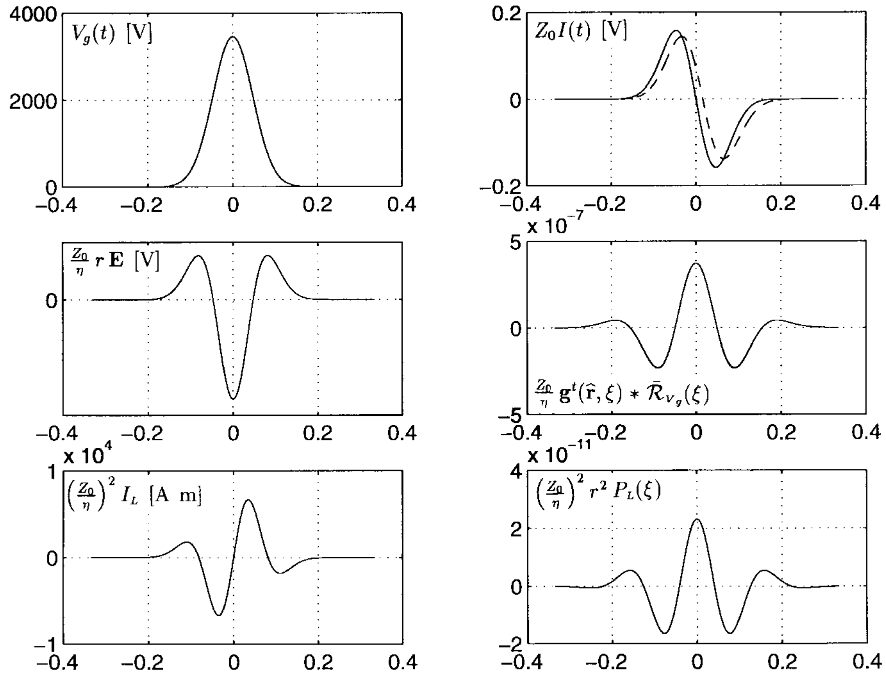

Fig. 6. Waveforms of the short-dipole example. The horizontal axis is the time in μs. (a) The driving pulse $V_g(t)$ of (37). (b) The normalized current $Z_0 I(t)$ of (40) at the antenna terminals. Two values of Z_0 are considered: $Z_0 = 50\ \Omega$ (full line) and $Z_0 = 5$ KΩ (dashed line). (c) The normalized radiated electric pulse $\frac{Z_0}{\eta}\, r\, \mathbf{E}$ of (42) for $\theta = \pi/2$. (d) The normalized transmitting antenna gain correlator $\frac{Z_0}{\eta}\, \mathbf{g}^t(\hat{\mathbf{r}}, \xi) * \bar{\mathcal{R}}_{V_g}(\xi)$ of (43) for $\theta = \pi/2$. (e) The normalized load current $(\frac{Z_0}{\eta})^2 I_L$ of (45) at the receiving antenna. (f) The normalized energy correlator $(\frac{Z_0}{\eta})^2 r^2\, P_L(\xi)$ of (46).

Applying the slant-stack transform (5) to the current distribution in (38), we obtain the effective transmission height as (see details in Appendix B)

$$\mathbf{h}^t(\hat{\mathbf{r}}, \tau) = -\hat{\boldsymbol{\theta}} \sin\theta \frac{L^2}{2c} \delta''(\tau). \tag{39}$$

Recall that the effective height is defined with the incident current wave as the reference [see (10)]. This operator provides the physical radiating pulse only if the input pulse is within the parameter range of the short-dipole approximation. It should be recalled that $\mathbf{J}^\delta$ in (38) is the antenna current due to forward propagating current pulse. The actual transmission line current due to the excitation $V_g(t)$ includes also the reflected pulse [see (24)]. From the transmitting antenna circuit in Fig. 1, neglecting R^{rad} in comparison to Z_0 for the short-dipole parameter range we obtain

$$I_{\mathrm{in}}(t) = \frac{V_g(t)}{Z_0}[1 - \sqrt{\pi}(T/\tau^t) F(T/\tau^t - t/2T)] \tag{40}$$

where $\tau^t = Z_0 C$ and the Fresnel function is defined as

$$F(x) = e^{x^2} \frac{2}{\sqrt{\pi}} \int_x^\infty e^{-u^2}\, du. \tag{41}$$

Equation (40) may also be calculated via the FD using the antenna reflection coefficient [see (63)]. Plots of the normalized current $I_{\mathrm{in}}(t)$ are shown in Fig. 6(b) for the dipole antenna whose dimensions have been specified above. Two cases are considered, one with $Z_0 = 50\ \Omega$ and the other for $Z_0 = 5$ KΩ. In the first, $\tau^t = 178$ ps $\ll T$, hence, the antenna current has approximately the form of a first order time-derivative of the driving voltage, while in the second, $\tau^t = 17.8$ ns. $\sim T$ causing a distortion of the input signal.

Next, by operating with (39) on (37) [see (12)] we obtain the radiated field

$$\mathbf{E}(\mathbf{r}, t) = \hat{\boldsymbol{\theta}} \sin\theta \frac{1}{16\pi r} \frac{\eta}{Z_0} \left(\frac{L}{2cT}\right)^2 H_2(\tau/2T) V_g(\tau) \qquad \tau = t - r/c \tag{42}$$

where H_n denotes the nth order Hermite polynomial. The resulting normalized waveform $\frac{Z_0}{\eta} r \mathbf{E}(\mathbf{r}, t)$, plotted in Fig. 6(c), is proportional to a second time-derivative of V_g, cf. (39).

The gain operator of the transmitting antenna is found from (17) using (39), giving

$$\mathbf{g}^t(\hat{\mathbf{r}}, \xi) = \hat{\boldsymbol{\theta}} \frac{\eta}{16\pi Z_0} \left(\frac{L}{c}\right)^4 \sin^2\theta\, \partial_\xi^4. \tag{43}$$

Fig. 6(d) depicts the normalized gain correlator $\frac{Z_0}{\eta} \mathbf{g}^t(\hat{\mathbf{r}}, \xi) * \bar{\mathcal{R}}_{V_g}(\xi)$ where for the pulse in (37)

$$\bar{\mathcal{R}}_{V_g}(\xi) = e^{-\frac{1}{8}\left(\frac{\xi}{T}\right)^2}. \tag{44}$$

Note that $\partial_\xi^4 \bar{\mathcal{R}}_{V_g}(\xi) = (1/\sqrt{8}T)^4\ H_4(\xi/\sqrt{8}T) \bar{\mathcal{R}}_{V_g}(\xi)$.

Next, we consider a transmit-receive dipole antennas system where, for simplicity, the two antennas have parallel axes and are thus polarization matched. Substituting in (31) [or (32)] we find the load current

$$I_L(t) = -\frac{1}{16\pi r} \frac{\eta}{4 Z_{0_T} Z_{0_R}} \frac{L_T^2 L_R^2}{(2cT)^3} \sin^2\theta H_3(\tau/2T) V_g(\tau) \tag{45}$$

where $Z_{0_{T,R}}$ and $L_{T,R}$ are the transmission-line impedances and lengths of the transmitting and receiving antenna, respectively, while θ is the relative angle between the antennas.

Note that this waveform is governed essentially by a third derivative of V_g. The normalized result $(\frac{Z_0}{\eta})^2 r I_L$ is depicted in Figs. 6(e). For simplicity we used the same parameters for the receiving antenna as those described previously for the transmitting antenna, namely $Z_0 = 50\ \Omega$ or $Z_0 = 5\ \text{K}\Omega$, $R_L = Z_0$, and $L_{T,R} = 1$ m. The current waveforms depicted are thus normalized as indicated in the figure. Finally, from (34) and (35) we calculate the transmission energy correlator

$$P_L(\xi) = -\mathcal{E}_g \left(\frac{1}{4\pi r}\right)^2 \frac{\eta^2}{Z_{0_T} Z_{0_R}} \frac{L_T^4 L_R^4}{(4\sqrt{2}cT)^6} \times \sin^4\theta H_6(\xi/\sqrt{8}T)\bar{\mathcal{R}}_{V_g}(\xi). \tag{46}$$

Expression (46) normalized by $(\frac{Z_0}{\eta})^2 r^2 \mathcal{E}_g^{-1} P_L$ is depicted in Fig. 6(f). From (33), the load energy $\mathcal{E}_L$ is given by $P_L(\xi = 0)$.

VI. Conclusion

The comprehensive characterization of antennas in the TD, presented herein, has been derived entirely in the context of the TD field equations. Central to the theory is the use of the SST that extracts the plane-wave spectrum of the time-dependent current distribution. Unlike the conventional FD circuit parameters, the TD circuit representation employs wave-type constituents [see e.g. I^+ in (8) and V^- in (20)]. Subject to this difference, the TD concepts and equations are equivalent to their commonly used FD counterparts via a temporal Fourier transform. For example, the TD gain operator is the autocorrelation of the transmitting effective height in response to an impulsive incident current; its transform coincides with the FD definition of the power gain, as alluded to in Appendix A below. This operator definition does not preclude, though, the use of stand-alone numerical concepts such as the "gain parameter" defined in Section II-D. The convolution operators in the transmit-receive equation (35) are translated into the products in the FD Friis operator (Appendix A). Convolution of (35) with the autocorrelation of the input signal (with $\xi = 0$) is transformed into a product of the Friis operator with the power spectrum, integrated over the entire frequency range. This allows for the evaluation of the far-field interaction between two antennas, characterized by their respective gain operators, given the excitation pulse such that both the received pulse shape and the power balance are obtainable, as demonstrated by the short-dipole example in Section V. It should be also noted that the operator representation enables the inclusion of additional elements within the transmit-receive system such as scattering objects, which would be characterized by cascaded operators in a manner similar to the antennas [23]. This work is now being extended to include pulsed-delay arrays (PDA's).

Appendix A
The Relation Between the Frequency- and Time-Domain Characterizations

In this section, we shall briefly comment on the relation between the TD formulation introduced in this paper and the conventional FD formulation. Henceforth, field constituents with over carets denote a FD constituent with an assumed time-dependence $e^{-i\omega t}$. The TD expressions are recovered from the corresponding FD expressions via

$$f(t) = \frac{1}{2\pi} \int_{-\infty}^{\infty} d\omega \hat{f}(\omega) e^{-i\omega t}. \tag{47}$$

A. The Slant-Stack Transform and the Fourier Transform

In the conventional FD formulation of the radiation problem, the far-field approximation for the vector potential $\hat{\mathbf{A}}(\mathbf{r},\omega)$ is given by

$$\hat{\mathbf{A}}(\mathbf{r},\omega) \sim \frac{e^{ikr}}{4\pi r} \mu \hat{\tilde{\mathbf{J}}}(\mathbf{K},\omega)|_{\mathbf{K}=k\hat{\mathbf{r}}} \tag{48}$$

where $k = \omega/c$, while r and $\hat{\mathbf{r}}$ have been defined in (2). Here

$$\hat{\tilde{\mathbf{J}}}(\mathbf{K},\omega) = \int dV' \hat{\mathbf{J}}(\mathbf{r}',\omega) e^{-i\mathbf{K}\cdot\mathbf{r}'} \tag{49}$$

is the spatial Fourier transform of the current at each frequency ω. To clarify the notations used throughout this paper, we note that an "over tilde" always describes the plane wave spectrum; thus, the notation $\hat{\tilde{}}$ describes a plane wave spectrum of time-harmonic fields as obtained by the $\mathbf{K}$ transform (49), whereas $\tilde{}$ describes the time-dependent plane wave spectrum as obtained from the SST in (5).

Transforming (48) to the TD via (47) yields

$$\mathbf{A}(\mathbf{r},t) = \frac{\mu}{4\pi r} \frac{1}{2\pi} \int_{\infty}^{\infty} d\omega \int dV' \hat{\mathbf{J}}(\mathbf{r}',\omega) e^{-i\omega(t - r/c + \hat{\mathbf{r}}\cdot\mathbf{r}'/c)}. \tag{50}$$

Changing the order of integration and integrating with respect to ω yields the slant-stack transform result in (4) and (5), which is formulated entirely in the TD.

B. The Transmitting Antenna Effective Height

The effective height is usually defined with respect to a receiving condition. However, we may define the FD transmitting antenna effective height via

$$\hat{\mathbf{E}}(\mathbf{r},\omega) = -\frac{e^{ikr}}{4\pi r} \mu \hat{I}(\omega) \hat{\mathbf{h}}^t(\hat{\mathbf{r}},\omega). \tag{51}$$

Note the FD effective height is defined with respect to the *total* terminal current $\hat{I}(\omega)$ whereas the TD definition (8) is defined with respect to the incident current pulse $I^+(t)$ [we use different symbols for $\mathbf{h}^t(t)$ and $\hat{\mathbf{h}}^t(\omega)$ to emphasize that these two parameters are not Fourier transform pair, cf. (53)]. One finds

$$\hat{\mathbf{h}}^t(\hat{\mathbf{r}},\omega) = -i\omega \hat{\tilde{\mathbf{J}}}_{\|}(\mathbf{K},\omega)|_{\mathbf{K}=k\hat{\mathbf{r}}} \tag{52}$$

where $\hat{\tilde{\mathbf{J}}}(\mathbf{K},\omega)$ is the $\mathbf{K}$ transform (49) of the current distribution $\hat{\mathbf{J}}(\mathbf{r},\omega)$ due to an input current with unit amplitude, and the subscript $_{\|}$ denotes the component of $\hat{\tilde{\mathbf{J}}}$ transverse to the observation direction $\hat{\mathbf{r}}$. Thus, in view of (10), and the analogy between the SST and the $\mathbf{K}$ transforms and also, since $\hat{I}(\omega) = \hat{I}^+(\omega)[1 - \hat{\Gamma}^t(\omega)]$, one finds that

$$\mathbf{h}^t(\hat{\mathbf{r}},t) \leftrightarrow [1 - \hat{\Gamma}^t(\omega)] \hat{\mathbf{h}}^t(\hat{\mathbf{r}},\omega). \tag{53}$$

where $\leftrightarrow$ symbolizes a Fourier transform relationship and $\hat{\Gamma}^t(\omega)$ is the reflection coefficient at the antenna terminals.

C. The Transmitting Antenna Gain

The FD definition of the transmitting antenna gain vector (i.e., including polarization—sometimes referred to as partial gain) is

$$\hat{\mathbf{g}}^t(\hat{\mathbf{r}},\omega)=\frac{\frac{1}{2}|\hat{\mathbf{E}}(\mathbf{r},\omega)|^2/\eta}{\hat{P}_{\text{in}}(\omega)/4\pi r^2}\hat{\mathbf{p}} \tag{54}$$

where $\hat{\mathbf{p}}\equiv\hat{\mathbf{E}}(\mathbf{r},\omega)/|\hat{\mathbf{E}}(\mathbf{r},\omega)|$ is the polarization vector. Note that in the FD $|\hat{\mathbf{E}}|\equiv\sqrt{\hat{\mathbf{E}}\cdot\hat{\mathbf{E}}^*}$. If in (54) the input power is taken to be $\hat{P}_{\text{in}}=\frac{1}{2}|\hat{V}_g|^2/4Z_0=\hat{P}^+$, then using (51) we obtain

$$\hat{\mathbf{g}}^t(\hat{\mathbf{r}},\omega)=\frac{1}{4\pi c^2}\frac{\eta}{Z_0}|\hat{\mathbf{h}}^t(\hat{\mathbf{r}},\omega)|^2\hat{\mathbf{p}}. \tag{55}$$

Comparing (55) and (17), we conclude that

$$\hat{\mathbf{g}}^t(\hat{\mathbf{r}},\omega)\leftrightarrow\mathbf{g}^t(\hat{\mathbf{r}},\xi). \tag{56}$$

Recall that $\mathbf{g}^t$ is the normalized gain (due to an impulsive excitation) used in (15) by convolving $\mathbf{g}^t$ with the normalized autocorrelation of the excitation waveform.

D. The Receiving Antenna Effective Height and Gain

In the FD, the receiving antenna effective height is conventionally defined via [compare (20)]

$$\hat{V}^{\text{oc}}(\omega)=-\hat{\mathbf{E}}_0(\omega)\cdot\hat{\mathbf{h}}^r(\hat{\mathbf{r}},\omega) \tag{57}$$

where $\hat{V}^{\text{oc}}$ is the open circuit voltage at the receiving antenna terminals, and

$$\hat{\mathbf{h}}^r(\hat{\mathbf{r}},\omega)=\hat{\hat{\mathbf{J}}}_{\|}(\mathbf{K},\omega)|_{\mathbf{K}=k\hat{\mathbf{r}}} \tag{58}$$

where $\hat{\hat{\mathbf{J}}}_{\|}$ has been defined in (52). As noted in connection with (51), we use different symbols for $\mathbf{h}^r(t)$ and $\hat{\mathbf{h}}^r(\omega)$ to emphasize that these two parameters are not a Fourier transform pair as the former is defined with respect to the traveling wave V^- whereas the latter is defined with respect to the total open circuit voltage $\hat{V}^{\text{oc}}$.

Recalling that our TD definition of the effective height in (20) involves the traveling wave voltage $V^-(t)$ obtained when the receiving antenna is connected to an infinitely long transmission line with characteristic impedance Z_0, and using $\hat{V}^-(\omega)=\frac{1}{2}[1-\hat{\Gamma}^t(\omega)]\hat{V}^{\text{oc}}(\omega)$ we obtain

$$\mathbf{h}^r(\hat{\mathbf{r}},t)\leftrightarrow\frac{1}{2}[1-\hat{\Gamma}^t(\omega)]\hat{\mathbf{h}}^r(\hat{\mathbf{r}},\omega). \tag{59}$$

Combining (52), (53), (58), and (59) we arrive at the TD reciprocity condition (29) which has been derived there using direct TD considerations.

E. The Transmit-Receive (Friis) Equation

Finally, it is instructive to demonstrate the relation of (35) to the FD Friis equation

$$\hat{P}_L(\omega)=\hat{P}_{\text{in}}(\omega)\frac{\hat{\mathbf{g}}_T^t(\hat{\mathbf{r}},\omega)\cdot\hat{\mathbf{g}}_R^t(\hat{\mathbf{r}},\omega)}{(4\pi r/\lambda)^2} \tag{60}$$

where $\hat{P}_{\text{in}}(\omega)$ is the power spectrum of the source while $\hat{\mathbf{g}}_{T,R}^t(\hat{\mathbf{r}},\omega)$ denote the FD gain of antenna T and R, respectively. The relation of this expression to the TD expression in (35) and (33) is readily established if we recast (60) as the transmission Friis operator

$$\hat{P}_L(\omega)=\hat{\mathcal{T}}(\omega)\hat{P}_{\text{in}}(\omega) \tag{61}$$

so that

$$\hat{\mathcal{T}}(\omega)=-\left(\frac{1}{4\pi r}\right)^2(2\pi c)^2\hat{\mathbf{g}}_T^t(\hat{\mathbf{r}},\omega)\cdot\hat{\mathbf{g}}_R^t(\hat{\mathbf{r}},\omega)(-i\omega)^{-2}. \tag{62}$$

Equations (62) and (61) are the transforms of the energy correlator (34) and the TD operator (35) with the individual constituents being the transforms of one another [recall (56) and also note that the input power spectrum $\hat{P}_{\text{in}}(\omega)$ in (61) is the transform of the input-energy correlator $\mathcal{E}_g\mathcal{R}_{V_g}(\xi)$ in (34)]. Upon integrating (61) over the entire frequency range, we arrive at (33).

F. The Short-Dipole System

The short-dipole system, treated in Section V can also be related to the FD expressions. Suppressing the time delay reference t_g in (11), the FD incident current wave is $\hat{I}^+(\omega)=\hat{V}_g/2Z_0$. The input current into the dipole is

$$\hat{I}_{\text{in}}(\omega)=(1-\hat{\Gamma}^t(\omega))\hat{I}^+(\omega)=\frac{-i\omega\tau^t}{1-i\omega\tau^t}\frac{\hat{V}_g(\omega)}{Z_0} \tag{63}$$

where we used $1-\hat{\Gamma}^t(\omega)=\frac{2Z_0}{Z_{\text{in}}+Z_0}$ with $Z_{\text{in}}=(-i\omega C)^{-1}$ and $\tau^t=Z_0C$ is defined in (41). The FD current over the short-dipole has a triangular distribution

$$\hat{\mathbf{J}}(z,\omega)=\hat{\mathbf{z}}\,2ik(|z|-L/2)\hat{I}^+(\omega). \tag{64}$$

Defining now the effective height with the *incident current* as a reference

$$\hat{\mathbf{h}}^t(\hat{\mathbf{r}},\omega)=\hat{\boldsymbol{\theta}}\frac{1}{2}(kL)^2C\sin\theta. \tag{65}$$

This FD expression is analogous to (39). However, as it is customary to define FD quantities with the *total* input current as the reference, (65) can be adapted via (59) to yield $\hat{\mathbf{h}}^t(\hat{\mathbf{r}},\omega)=\hat{\mathbf{h}}^t(\hat{\mathbf{r}},\omega)/(1-\hat{\Gamma}^t(\omega))$ where as noted after (63), $1-\hat{\Gamma}^t(\omega)=\frac{-2i\omega\tau^t}{1-i\omega\tau^t}$.

Appendix B
TD Antenna Length Calculations

In this section, the SST (5) is applied to the current distribution in (38) to derive expression (39) for the effective height operator of a short dipole. We consider first the contribution of the current distribution at $0<t<\frac{L}{2c}$. Performing the integration $\int dV'\mathbf{J}_{\|}^{\delta}(\mathbf{r}',\tau+\hat{\mathbf{r}}\cdot\mathbf{r}'/c)$ in (10), yields for the upper arm of the dipole

$$\begin{aligned}&-\hat{\boldsymbol{\theta}}\sin\theta\int_0^{L/2}dz'\delta\left(\tau-\frac{z'}{c}(1-\cos\theta)\right)\\&\quad=-\hat{\boldsymbol{\theta}}\frac{c\sin\theta}{1-\cos\theta}\left[H(\tau)H\left(\tau-\frac{L}{2c}(1-\cos\theta)\right)\right]\end{aligned} \tag{66}$$

and for the lower arm

$$\begin{aligned}&-\hat{\boldsymbol{\theta}}\sin\theta\int_{-L/2}^{0}dz'\delta\left(\tau+\frac{z'}{c}(1+\cos\theta)\right)\\&\quad=-\hat{\boldsymbol{\theta}}\frac{c\sin\theta}{1+\cos\theta}\left[H(\tau)-H\left(\tau-\frac{L}{2c}(1+\cos\theta)\right)\right]\end{aligned}\tag{67}$$

where θ is the spherical angle with respect to the z axis and $\boldsymbol{\theta}$ is a unit vector in the θ direction. Following the same procedure for the time interval $\frac{L}{2c}<t<\frac{L}{c}$ and summing up the results we obtain

$$\begin{aligned}&\int dV'\mathbf{J}_{\|}^{\delta}(\mathbf{r}',\tau+\hat{\mathbf{r}}\cdot\mathbf{r}'/c)\\&\quad=-\hat{\boldsymbol{\theta}}\frac{2c\sin\theta}{1-\cos^2\theta}\left[H(\tau)+H\left(\tau-\frac{L}{c}\right)\right.\\&\qquad\left.-H\left(\tau-\frac{L}{2c}(1-\cos\theta)\right)-H\left(\tau-\frac{L}{2c}(1+\cos\theta)\right)\right].\end{aligned}\tag{68}$$

Differentiating (68) with respect to τ and convolving it with the input current pulse $I(t)$, we obtain

$$\begin{aligned}&\mathbf{h}^t(\hat{\mathbf{r}},\tau)*I(t)\\&\quad=-\hat{\boldsymbol{\theta}}\frac{2c\sin\theta}{1-\cos^2\theta}\left[I(\tau)+I\left(\tau-\frac{L}{c}\right)\right.\\&\qquad\left.-I\left(\tau-\frac{L}{2c}(1-\cos\theta)\right)-I\left(\tau-\frac{L}{2c}(1+\cos\theta)\right)\right].\end{aligned}\tag{69}$$

The waveforms in (69) have the general form $I(\tau+\alpha)$ where α is proportional to L/c, hence, utilizing the fact that $cT\gg L$ we may approximate these waveforms as Taylor series about τ in the form $I(\tau+\alpha)=I(\tau)+\alpha I'(\tau)+\frac{1}{2}\alpha^2I''(\tau)$. The zeroth and the first-order terms cancel out, leaving the second order term

$$\mathbf{h}^t(\hat{\mathbf{r}},\tau)*I(t)=-\hat{\boldsymbol{\theta}}\sin\theta\frac{L^2}{2c}I''(\tau)\tag{70}$$

and thus proving (39). Note that this expression is the TD counterpart of the effective height of a time-harmonic short-dipole antenna. Assuming $kL\ll 1$, the current along such antenna has the triangular distribution $\hat{\mathbf{J}}=\mathbf{z}(1-2|z|/L)e^{i\omega t}$, giving via (52) the well-known effective height $\hat{\mathbf{h}}^t(\hat{\mathbf{r}},\omega)=(kL)^2\frac{c}{2}\hat{\boldsymbol{\theta}}\sin\theta$.

References

[1] L. Carin and L. B. Felsen, Eds., *Ultra-Wideband Short-Pulse Electromagnetics*. New York: Plenum, 1995.
[2] G. Franceschetti and C. H. Papas, "Pulsed antennas," *IEEE Trans. Antennas Propagat.*, vol. AP-22, pp. 651–661, Sept. 1974.
[3] M. Sato, M. Iguchi, and R. Sato, "Transient response of coupled linear dipole antennas," *IEEE Trans. Antennas Propagat.*, vol. AP-32, pp. 133–140, Feb. 1984.
[4] D. M. Pozar, R. E. McIntosh, and S. G. Walker, "The optimum feed voltage for a dipole antenna for pulse radiation," *IEEE Trans. Antennas Propagat.*, vol. AP-31, pp. 563–569, July 1983.
[5] D. M. Pozar, D. H. Schaubert, and R. E. McIntosh, "The optimum transient radiation from an arbitrary antenna," *IEEE Trans. Antennas Propagat.*, vol. AP-32, pp. 633–640, June 1984.
[6] D. M. Pozar, Y. W. Kang, D. H. Schaubert, and R. E. McIntosh, "Optimization of the transient radiation from a dipole array," *IEEE Trans. Antennas Propagat.*, vol. AP-33, pp. 69–75, Jan. 1985.
[7] Y. W. Kang and D. M. Pozar, "Optimization of pulse radiation from dipole array for maximum energy in specified time interval," *IEEE Trans. Antennas Propagat.*, vol. AP-34, pp. 1383–1386, Dec. 1986.
[8] J. P. R. Bayard and D. H. Schaubert, "Transient response of receiving dipole array: Bounds and maximization," *IEEE Trans. Electromagn. Compat.*, vol. 30, pp. 122–129, 1988.
[9] C. E. Baum, "General properties of antennas," *Sensor Simulat. Notes*, Note 330, 1991.
[10] C. R. Baum and E. G. Farr, "Extending the definitions of antennas gain and radiation pattern into the time domain," *Sensor Simulat. Notes*, Note 350, 1992.
[11] G. F. Farr and C. E. Baum, "Impulse radiating antennas," in *Ultra-Wideband Short-Pulse Electromagnetics*, H. L. Bertoni, L. Carin, and L. B. Felsen, Eds. New York: Plenum, 1994, pp. 139–147.
[12] G. F. Farr, C. E. Baum, and C. J. Buchenauer, "Impulse radiating antennas: Part II," in *Ultra-Wideband Short-Pulse Electromagnetics*, L. Carin and L. B. Felsen, Eds. New York: Plenum, 1995, pp. 159–170.
[13] R. W. Ziolkowski, "Properties of electromagnetic beams generated by ultra-wide bandwidth pulse-driven arrays," *IEEE Trans. Antennas Propagat.*, vol. 40, pp. 888–905, Aug. 1992.
[14] O. E. Allen, D. A. Hill, and A. R. Ondrejka, "Time domain antennas characterization," *IEEE Trans. Electromagn. Compat.*, vol. 35, pp. 339–345, 1993.
[15] D. Lamensdorf and L. Susman, "Baseband-pulse-antenna techniques," *IEEE Antennas Propagat. Mag.*, vol. 36, pp. 20–30, Feb. 1994.
[16] H. W. Lorber, "A time domain radar range equation," in *Ultra-Wideband Short-Pulse Electromagnetics*, L. Carin and L. B. Felsen, Eds. New York: Plenum, 1995, pp. 355–364.
[17] T. B. Hansen and A. D. Yaghjian, "Planar near field scanning in the time domain—Part I: Formulation," *IEEE Trans. Antennas Propagat.*, vol. 42, pp. 1280–1291, Sept. 1994.
[18] ——, "Part II: Sampling theorem and computation schemes," *IEEE Trans. Antennas Propagat.*, pp. 1292–1300, Sept. 1994.
[19] E. Heyman and T. Melamed, "Certain consideration in aperture synthesis for ultra-wideband/short-pulsed fields," *IEEE Trans. Antennas Propagat.*, vol. 42, pp. 518–525, Apr. 1994.
[20] E. Heyman, "Time-dependent plane-wave spectrum representations for radiation from volume source distributions," *J. Math. Phys.*, vol. 37, pp. 658–681, 1996.
[21] W. J. Welch, "Reciprocity theorem for electromagnetic fields whose time dependence is arbitrary," *IRE Trans. Antennas Propagat.*, vol. AP-8, pp. 70–73, Jan. 1960.
[22] L. B. Felsen and N. Marcuvitz, *Radiation and Scattering of Waves*. Englewood Cliffs, NJ: Prentice Hall, 1973.
[23] E. C. Jordan and K. G. Balmain, *Electromagnetic Waves and Radiation Systems*. Englewood Cliffs, NJ: Prentice Hall, 1968.

Amir Shlivinski (M'93) was born in Tel-Aviv, Israel, in February 1969. He received the B.Sc. degree (*cum laude*) and the M.Sc. degree in electrical engineering, both from Tel-Aviv University, Israel, in 1991 and 1997, respectively.

His main fields of interest are electromagnetic and antenna theory, wave theory, and time-domain phenomena.

Ehud Heyman (S'80–M'82–SM'88), for photograph and biography, see p. 528 of the May 1995 issue of this TRANSACTIONS.

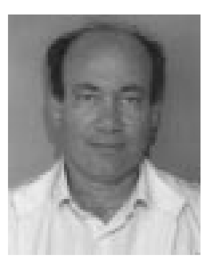

Raphael Kastner (S'80–M'82–SM'87) received the B.S. (*summa cum laude*) and M.S. degrees from the Technion, Israel Institute of Technology, Haifa, in 1973 and 1976, respectively, and the Ph.D. degree from the University of Illinois, Urbana-Champaign, in 1982.

From 1976 to 1988 he was with RAFAEL, Israel Armament Development Authority, Haifa, where from 1982 to 1986 he headed the antenna section. He was a Visiting Assistant Professor at Syracuse University, Syracuse, New York, from 1986 to 1987 and a Visiting Scholar at the University of Illinois, Urbana-Champaign, in 1987 and 1989. Since 1988 he has been with the Department of Physical Electronics, Tel Aviv University, where he is now an Associate Professor. He is on the editorial board for the *Journal of Electromagnetic Waves and Applications*.

Dr. Kastner is a member of Tau Beta Pi, Eta Kappa Nu, and URSI Commission B. He has served as the Treasurer of the IEEE Israel Section.